ISSN: 2414-1895 DOI: 10.6919/ICJE.202506_11(6).0021

Study on the Characteristics of Fractured Rock Cracking and the Precursors of Instability

Yantao Yu, Yuan Chang*, Yunyu Li, Shuyi Zhou, Mengyuan Zhou, Yulin Yang

School of Civil Engineering, Liaoning University of Science and Technology, Anshan, China

Abstract

In the fields of geology, mining, and hydropower engineering, the cracking and instability of fractured rocks pose a serious threat to project safety. This paper conducts uniaxial compression tests on rectangular sandstone samples containing pre-formed through-and-apart fractures, using advanced equipment to collect data and processing it with ORIGIN and MATLAB software to obtain acoustic emission stress-strain curves and grayscale images to record fracture propagation. The study finds that the failure of fractured sandstone samples is influenced by both wing cracks and secondary cracks, with the stress-strain curve divided into four stages, exhibiting brittle failure characteristics. Acoustic emission signals show different features at various deformation stages, characterized by dense signals and cumulative vibration The increase of bell count and the "step-like" change of stress-strain curve are the precursors of failure. The grayscale image and curve generated based on MATLAB can also reflect the crack propagation, and the abnormal change of grayscale value is also a precursor of failure, which provides a basis for related research.

Keywords

Fractured Rock; Acoustic Emission; Cracking Precursors.

1. Introduction

Nowadays, large-scale engineering projects are thriving, but the accompanying engineering issues are also on the rise. For instance, in fields such as geological engineering, mining engineering, and hydropower engineering, the cracking and instability of fractured rocks have become increasingly prominent, posing significant challenges to construction. Therefore, studying the mechanical behavior of fractured rock masses, the evolution of cracks, and their disaster-causing mechanisms is of great practical significance for predicting and controlling rock mass instability[1]. In order to study the influence of fractured rocks on engineering construction, scholars at home and abroad have done a lot of research work. In terms of indoor experiments, a large number of scholars[1-6]The uniaxial compression tests were conducted on specimens such as single-fracture rocks with different inclinations, and the failure processes were thoroughly studied. The impact of different fracture angles on the initiation, propagation, and failure modes of fractured sandstone samples was analyzed. However, the instability and failure of rock masses are often influenced by multiple fractures within them，Therefore, some scholars[7-9]A series of studies on rocks containing multiple fractures have been carried out, and it is found that multiple fractures dominate the crack propagation of rocks. The fracture tips and the edges of holes crack first to form a network of fractures, and the holes and fractures cooperate to aggravate the rock mass destructionLiang et al.[10]conducted quasi-static compression tests on fractured sandstone under FT cycles, using acoustic emission monitoring and digital image correlation systems to capture failure characteristics. The results show that FT cycles and fracture angles influence failure modes by increasing internal structural defects and affecting the geometric distribution of stress conditions, respectively.Li et al. [11]studied the strength and damage

ISSN: 2414-1895 DOI: 10.6919/ICJE.202506_11(6).0021

characteristics of rock masses under true triaxial unloading conditions with different crack inclinations, analyzing the impact of path on the extension patterns of cracks. Nataf et al. [12]conducted uniaxial compression acoustic emission tests on different sandstones, finding that the loading rate has little effect on the power-law behavior of specimen compression failure, verifying the scale-free distribution of acoustic emissions in brittle failure of sandstone, and that inclination affects the strength and deformation characteristics of rocks.This study conducted uniaxial compression tests on rectangular sandstone samples containing fractures, using advanced equipment to collect data and processing it with ORIGIN and MATLAB software. The results obtained include acoustic emission stress-strain curves and grayscale images, clearly demonstrating the complete process of rock samples under uniaxial compression loading from compression to failure, highlighting the characteristics of fractured rocks before rupture. This research is significant for preventing safety hazards caused by rock fracture in actual engineering projects and ensuring the stability of structural engineering, providing robust data support and theoretical basis for design, construction, and maintenance of engineering projects.

2. The Test Process

2.1 Preparation of Fractured Rock Specimens

Select sandstone blocks with uniform lithology and no macroscopic defects, and cut them into two rectangular prisms using a high-precision rock cutter. Polish the blocks to a size of 50mm × 25mm × 100mm. At the pre-set fracture locations, drill a row of small holes that are 20mm long, 1mm wide, and at a 45-degree angle. Insert split wedges to apply external force, creating fractures. Next, use grinding and polishing equipment to treat the surface of the specimens, ensuring their flatness and smoothness meet the standards. Finally, conduct a comprehensive inspection using an ultrasonic detector. Only specimens that pass all tests can be used for subsequent research.

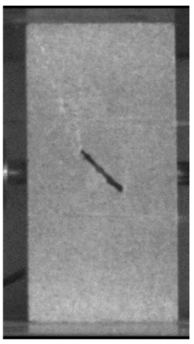

Figure 1. Sandstone samples with fractures of 45° inclination Angle R-SY3-LX

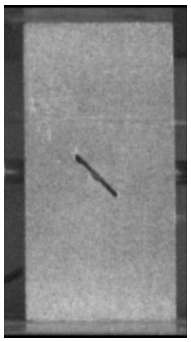

Figure 2. Sandstone samples with fractures of 45°inclination Angle R-SY5-LX

2.2 Specimen Size

Two samples with identical material and dimensions were prepared, numbered R-SY3-LX and R-SY5-LX. Each sample measures 50mm in length, 25mm in width, and 100mm in height, and contains

ISSN: 2414-1895 DOI: 10.6919/ICJE.202506_11(6).0021

a crack measuring 20mm in length and 1mm in width. These two specimens will be used for uniaxial compression testing. The measured inclination angle of the crack is determined using the following method: the bottom surface of the sandstone sample serves as the reference plane, and the angle formed between the pre-set crack face and the bottom surface of the sample is measured. This angle represents the measured inclination angle of the crack. Detailed dimensional parameters of the samples are shown in Table 1.

Table 1. Basic shape parameters of the sandstone samples

Sample number	Lithotomy Angle/(°)	Measured Angle/(°)	crack length /mm	Fracture width/mm
R-SY3-LX	45	46	20.6	1.2
R-SY5-LX	45	44.3	19.7	1.1

2.3 Experimental Installation; Laboratory Equipment

2.3.1 Single Axis Compression Testing Machine

The single-axis compression testing equipment used in this experiment is the YAD-2000 microcomputer-controlled electro-hydraulic servo pressure testing machine, as shown in Figure 3. This testing machine has a maximum loading pressure of 2000 KN, with an effective measurement range of 2% to 100%, and the piston movement speed is ≥45 mm/min. The testing system consists of a pressure application host, hydraulic source, electro-hydraulic servo controller, and electronic computer. The control method is force control loading. Before the test, a pre-load of 100N is applied, followed by continuous loading at a constant rate of 200 N/s until the sample is completely destroyed.

Figure 3. Uniaxial compression testing machine system[11]

2.3.2 Acoustic Emission Monitoring System

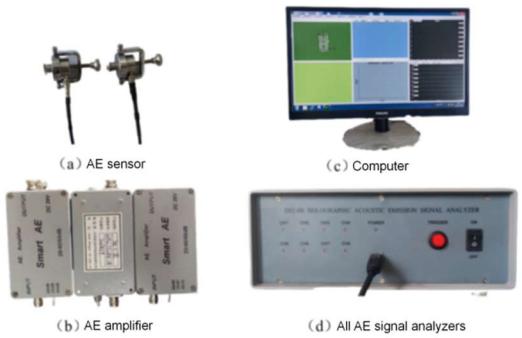

Figure 4. AE monitoring system[11]

This experiment used the DS2 type acoustic emission instrument to collect acoustic emission data from the specimen during loading. The data includes: ringing count, amplitude, energy rate, and peak frequency. The system operates stably with high sensitivity. As shown in Figure 4, the acoustic

ISSN: 2414-1895 DOI: 10.6919/ICJE.202506_11(6).0021

emission monitoring system consists of an electronic computer, a preamplifier, an AE sensor, and a holographic acoustic emission signal analyzer.

2.3.3 Experimental Procedure

Conducting uniaxial compression experiments on fractured rock, the preparatory work is extremely critical. When setting up acoustic emission sensors, they should be attached at the diagonal, antidiagonal, and center of the specimen, as well as 5mm away from the z-axis and y-axis edges, with clear division of labor to ensure comprehensive coverage of the rock surface. Apply Vaseline to the contact area between the sensor and the specimen to ensure tight contact and improve signal acquisition accuracy. Based on the characteristics of the rock and the experimental objectives, carefully configure the acoustic emission system parameters to ensure comprehensive capture of effective AE signals and minimize experimental result bias. Place a high-speed camera in a safe and well-visioned position next to the uniaxial compressor to clearly record the entire process from specimen compression to failure, providing visual data for subsequent research. After all preparations are completed, carefully check if the computer, acoustic emission system, and other equipment are functioning properly. Confirm everything is correct before starting the uniaxial compressor and the test control device, applying axial loads to the specimen steadily according to the loading plan. During the experiment, monitor data and changes in the specimen's appearance in real-time and record them to gather materials for analyzing rock mechanical properties.

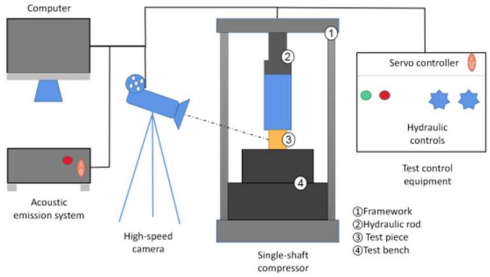

Figure 5. Schematic diagram of the working principle of the experimental system

3. Experimental Results and Analysis

3.1 Macroscopic Deformation and Destruction Characteristics of Fractured Rocks

For the R-SY3-LX sample, during loading, wing cracks formed at the crack tips, gradually extending parallel to the loading direction towards the center of the sample. At the same time, crack propagation was observed in the middle of the cracks, indicating an expanding stress concentration area, as shown in Figure 6. As loading continued, the cracks in the R-SY3-LX sample gradually expanded and eventually formed a through-crack, leading to overall failure of the sample. For the R-SY5-LX sample, multiple wing cracks and secondary cracks also appeared at the ends of the pre-existing cracks. During crack propagation, they moved towards the center of the sample, revealing a complex crack network. The crack propagation path in the R-SY5-LX sample was more complex, with cracks trending almost parallel to the loading direction, ultimately forming a main crack in the center of the sample, causing overall failure, as shown in Figure 7. In terms of failure morphology, the combined effect of wing cracks and secondary cracks led to the overall failure of the rock sample. The propagation paths and morphology of these cracks reflect the distribution and evolution of stress within the sample, providing important insights into the failure mechanisms of fractured sandstone and the cracking characteristics and pre-stable states of fractured rocks.

ISSN: 2414-1895 DOI: 10.6919/ICJE.202506_11(6).0021

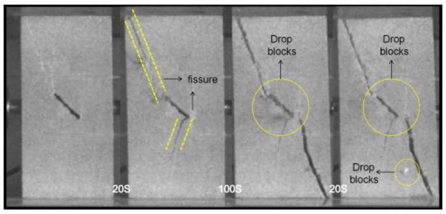

Figure 6. Fracture process of R-SY3-LX fractured sandstone sample

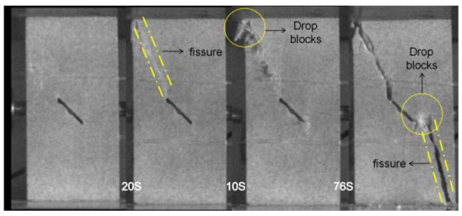

Figure 7. Fracture process of R-SY5-LX fractured sandstone sample

3.2 Test Results of Fractured Rocks

3.2.1 Stress-strain Relationship

The variability of rock samples can lead to fluctuations in test results. To eliminate this variability, samples of the same type were selected for comparative analysis, and a set was chosen where the destruction process could be clearly observed in the images. The stress-strain relationship of the fractured sandstone sample R-SY5-LX is shown in Figure 8. It can be seen that the stress-strain curve of this rock sample has a typical shape: the initial segment shows a concave bending pattern with relatively slow growth, during which the micro-pores and micro-cracks within the rock gradually become compacted; then it presents a step-like pattern, developing nearly linearly, with the duration of this phase gradually shortening as loading continues; followed by plastic deformation reaching a peak quickly before sharply declining, indicating complete failure due to the formation of through-cracks. Thus, the stress-strain curve of the rock can be roughly divided into four stages: ① initial compaction; ② linear elastic deformation stage; ③ plastic deformation stage; ④ rapid overall failure stage. The first two stages last longer, while the last two stages are shorter, showing clear characteristics of brittle failure. Taking the R-SY5-LX sample as an example, the division of the four stages in its stress-strain curve is shown in Figure 9. From the images of the destruction process, the expansion and evolution of fractures in the fractured rock during loading can be observed. Fractures typically start from initial defects and extend as the load increases, eventually leading to the overall fracture of the sample. Before fracture, the expansion rate of fractures may accelerate, with significant stress concentration in local areas, indicating that the material is about to enter a state of instability.

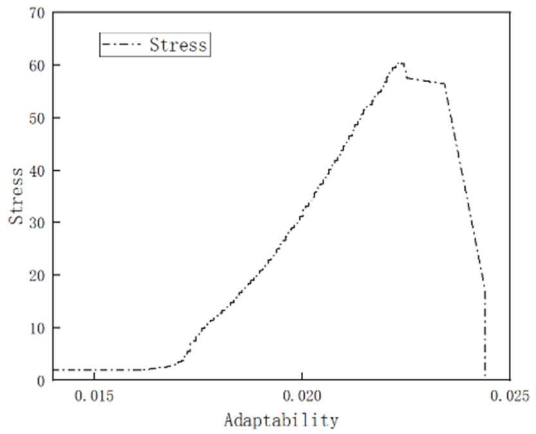

Figure 8. Stress-strain curve of fractured sandstone sample R-SY5-LX

ISSN: 2414-1895 DOI: 10.6919/ICJE.202506_11(6).0021

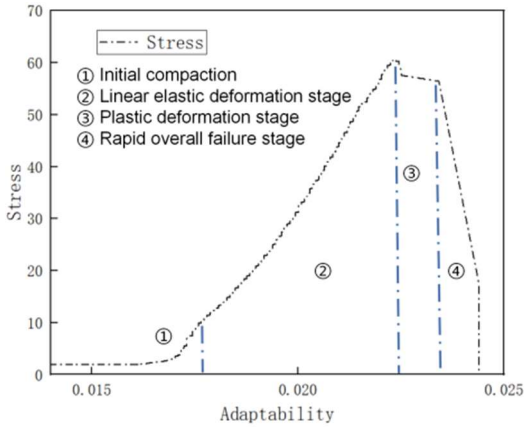

Figure 9. Stress-strain curve of R-SY5-LX fractured sandstone samples and the division of each stage

3.2.2 Sound Emission Test Results

The acoustic emission has the characteristics of synchronous with the mechanical parameters, and the acoustic emission characteristics of different deformation stages of rock are different[14]. uniaxial compression [15]Under load, The acoustic emission ringing count of pre-fractured rock and the relationship between stress and time can be thoroughly analyzed in conjunction with Figures 10 and 11. The product of the loading rate and time, divided by the sample height, yields the axial strain. As shown in Figure 10, the acoustic emission process from sand samples to complete failure is divided into three stages: ① Calm Period (Stage I): Initially, the rock sample is subjected to force, with rare acoustic emissions and a slow increase in cumulative ringing counts. Internal micro-pores and micro-cracks close, releasing only minor elastic waves without large-scale fractures, corresponding to the initial compaction segment and linear elasticity pre-stage of the stress-strain curve. ② Development Period (Stage II): Continuous loading leads to a dramatic increase in acoustic emissions, dense local signals, and a sharp rise in cumulative ringing counts. New micro-cracks form and propagate at the fracture tips, corresponding to the linear elasticity post-stage of the stress-strain curve. ③ Peak Period (Stage III): The rock sample approaches rupture, with extremely dense acoustic emission signals and a slightly gentle slope but with a "steep increase point" in the cumulative ringing count curve. Extensive internal fractures and micro-cracks penetrate, leading to rock failure, corresponding to the plastic deformation and overall failure stage of the stress-strain curve.

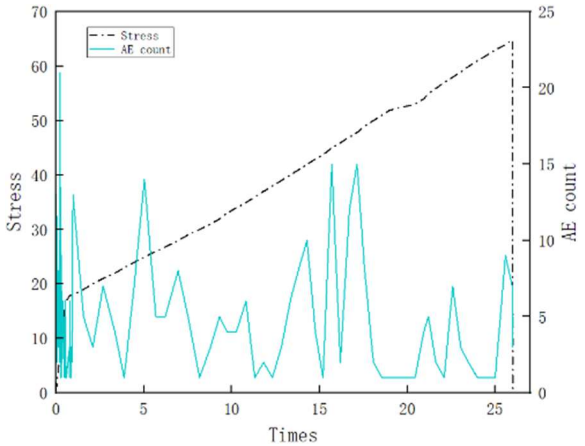

Figure 10. Relationship between acoustic emission bell ringing count, stress and loading time of R-SY3-LX fractured sandstone samples

ISSN: 2414-1895 DOI: 10.6919/ICJE.202506_11(6).0021

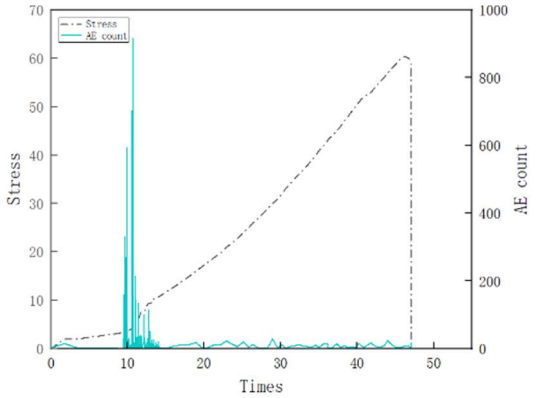

Figure 11. Relationship between acoustic emission bell ringing count, stress and loading time of fractured sandstone samples R-SY5-LX

3.2.3 The Image Analysis of the Precursor Was Obtained by Drawing the Grayscale Value Obtained by MATLAB Image Processing Technology

The grayscale images generated using MATLAB image processing technology[16] are highly valuable for studying the failure process of fractured sandstone samples R-SY3-LX. As shown in Figure 13, the vertical axis records the fracture area at a scale of ×10^6 pixels, finely depicting its changes. In terms of time, within 0-5 seconds, the development of internal fractures in the rock is slow, with a steady curve trend; from 5 to 10 seconds, fractures rapidly extend, causing the curve to sharply rise. During this stage, a large number of internal fractures form, expand, and connect, leading to rapid damage accumulation and a gradual decrease in load-bearing capacity, marking the critical warning period for macroscopic failure; after 10 seconds, the rate of fracture expansion slows down, and the curve stabilizes. At this point, a complex fracture network has been established within the rock, placing it in a state of critical failure or partial failure, where even slight external disturbance could result in complete disintegration.

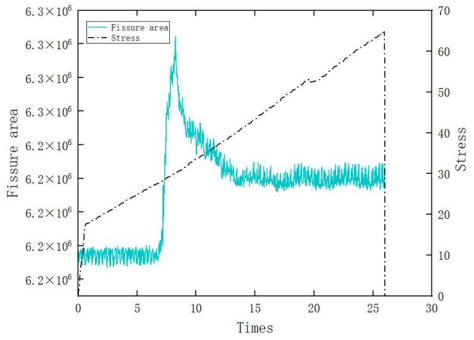

Figure 12. Image of the grayscale value during the fracture sandstone sample destruction process of R-SY3-LX

As shown in Figure 12, the grayscale-time curve generated based on MATLAB image processing technology vividly illustrates the dynamic evolution of the fractured sandstone sample R-SY5-LX during its failure process. Initially, from 0 to 20 seconds, the curve is nearly horizontal within the pixel range of 6.12×10^6 to 6.14×10^6, with almost no change in fracture area. The internal fractures of the rock are stagnant, and it is in a relatively stable elastic deformation stage. Immediately following, from 20 to 30 seconds, the curve sharply rises, with the fracture area increasing dramatically from about 6.14×10^6 pixels to nearly 6.26×10^6 pixels. During this phase, internal fractures rapidly sprout, expand, and interconnect like sparks spreading across a field, leading to a sharp accumulation of damage and a rapid decline in load-bearing capacity. The internal structure transitions abruptly from a stable state to a precarious one, marking a critical warning stage for impending macroscopic failure. In the subsequent 30 to 50 seconds, the curve fluctuates frequently,

ISSN: 2414-1895 DOI: 10.6919/ICJE.202506_11(6).0021

maintaining a relatively high fracture area but gradually decreasing and stabilizing. This is because after large-scale expansion, the internal fracture network enters a complex adjustment and reorganization phase, where new and old fractures compete with each other. At this point, the rock has established a complex fracture system, significantly reducing its load-bearing capacity and placing it on the brink of critical failure. Even minor external disturbances could cause complete disintegration. This curve, through dynamic tracking of surface grayscale values, clearly reveals the entire process of progressive failure in fractured rocks, from initial stability of fractures, rapid expansion leading to increased damage, to complex adjustments in the internal fracture network. The accelerated decline in grayscale values, changes in fluctuation patterns, and variations at key nodes are all important signs of impending failure.

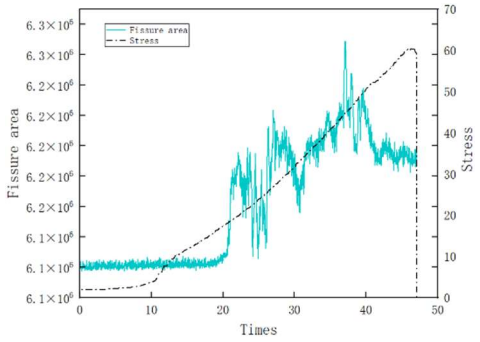

Figure 13. Image of the grayscale value during the fracture sandstone sample test in R-SY5-LX

4. Conclusion

(1) The uniaxial compression test was carried out on the fractured sandstone samples, and the acoustic emission monitoring was used to analyze the cracking characteristics and pre-damage precursors of the fractured rock in the whole process of damage. The following conclusions were drawn from the results:The stress-strain curve of fractured rock is divided into four stages, showing brittle failure. It presents a "step-like" pattern accompanied by dense acoustic emission signals, indicating internal fractures. In the early stage of loading, acoustic emissions are calm; during the development phase, they increase dramatically, reaching a peak close to rupture. These acoustic emission characteristics and curve states are important precursors to rock cracking and instability.

(2) In the study of fractured rocks, AE ringing counts images can clearly show their cracking characteristics and pre-decay. In the early loading stage, the internal structure of the rock closes, and the ringing count increases slowly, remaining relatively stable; during loading, new micro-cracks form and expand, causing a sharp increase in ringing count; as near rupture approaches, fractures occur frequently, resulting in "steep increases" in the ringing count curve, with dense signals. These are key indicators of rock instability.

(3) When loading fractured rocks, the grayscale image can intuitively show the precursors of cracking and failure. During the elastic deformation stage, the grayscale curve is stable, with slow crack development; during the damage acceleration stage, the curve surges sharply, leading to extensive crack initiation and propagation; as failure approaches, the curve fluctuates, either declining overall or stabilizing, with a complex internal fracture network. Changes in grayscale distribution, dynamic evolution, and statistical characteristics are all signs of impending failure.

References

[1] Wang Chengcheng, Luo Xinyao, Chen Kexu, et al. Experimental study on the evolution and rupture characteristics of rock fractures containing pre-fracture [J]. Gold Science & Technology, 2020,28(03): 421-429.

ISSN: 2414-1895 DOI: 10.6919/ICJE.202506_11(6).0021

[2] Li Xiulei, Xie Fei, Chen Chen, et al. Study on the Crack Propagation Behavior of Open Single Fracture Rocks Based on Acoustic Emission [J]. Hydrogeology and EngineeringGeology,2024,51(03):90-101.DOI:10.16030/j.cnki.issn.1000-3665.202303044.

[3] Wang Weihua, Wang Xiaojin, Jiang Haitao et al. Mechanical properties of rock-like samples with different dip angles under uniaxial compression [J]. Science and Technology Herald, 2014,32 (Z2):48-53.

[4] Hu Qianting, Yu Changjun, Li Quangui, et al. Experimental study on macroscopic and microscopic damage characteristics of fractured sandstone under uniaxial compression [J]. Experimental Mechanics, 2025,40(01):49-60.

[5] Li Chenpu, Xue Xiaoqiang, Tan Bingyan. Study on the Mechanism of Fracture in Rock under Biaxial Cyclic Load [C]// Structural Engineering Committee of Chinese Society of Theoretical and Applied Mechanics, Liaoning Technical University, Editorial Board of "Engineering Mechanics" of Chinese Society of Theoretical and Applied Mechanics, Department of Civil Engineering, Tsinghua University, National Key Laboratory of Hydrogeology and Hydraulic Engineering. Proceedings of the 33rd National Conference on Structural Engineering (Volume I). School of Environment and Civil Engineering, Chengdu University of Technology; 2024:10.DOI:10.26914/c.cnkihy.2024.023337.

[6] Ma Pengfei, Li Shuchen, Zhou Huiying, et al. Improved near-field dynamics method for crack propagation simulation of rock materials [J]. Rock and Soil Mechanics, 2019,40(10):4111-4119.DOI:10.16285/j.rsm.2018.1371.

[7] Liu Xianghua, Zhang Ke, Zhang Kai, et al. Fracture and fractal evolution of rock mass with multiple fractures in porous formations [J]. Journal of Underground Space and Engineering, 2021,17(04):1021-1027.

[8] Wu Xu, Guo Yuming, Sun Jinglai, et al. Energy evolution law of orthorhombic fractured rocks under uniaxial compression [J]. Journal of Underground Space and Engineering, 2021,17(S1):114-119.

[9] Zhang Ke, Liu Xianghua, Li Kun, et al. Study on the correlation between mechanical properties and fractal dimension of porous fractured rocks [J]. Journal of Rock Mechanics and Engineering, 2018,37(12):2785-2794.DOI:10.13722/j.cnki.jrme.2018.0894.

[10] Liang X ,Liu Z ,Peng K , et al.Failure prediction of fissured rock under freeze-thaw cycles based on critical slowing down theory of acoustic emission multi-parameter[J].Results in Engineering,2025,25103874-103874.

[11] Li W ,Gao Z ,Feng G , et al.Damage characteristics and YOLO automated crack detection of fissured rock masses under true-triaxial mining unloading conditions[J].Engineering Fracture Mechanics,2025,314110790-110790.

[12] Song Shuo. Study on Macroscopic and microscopic anchoring characteristics of coal-rock composite with prestressed anchor rods [D]. Liaoning University of Science and Technology, 2023.DOI:10.26923/d.cnki.gasgc.2023.000740.

[13] Chen Yike, Hu Shuting, Zhou Jiajun, et al. Study on acoustic emission characteristics of sandstone under uniaxial compression [J]. Engineering and Experiment, 2016,56(02):19-22+64.

[14] Dong Zehua, Wang Kaichuang, Jing Chuan, et al. Uniaxial compressive fatigue life of high strain hardened cementitious composites [J/OL]. Journal of CompositesScience,1-10[2025-04-14].https://doi.org/10.13801/j.cnki.fhclxb.20250305.005.

[15] Zhang Long.Matlab Application analysis of image enhancement technology [J]. Home Cinema Technology, 2024, (06):68-71.

[16] Xue Rui-xiong, Kong Ying-hui, Feng Jin-xiang. Study on fracture characteristics and instability precursors of different rocks based on acoustic emission [J]. Coal Technology, 2024,43(12):13-19.DOI:10.13301/j.cnki.ct.2024.12.003.